Quantitative Evaluation of d–π Interaction in Copper(I) Complexes and Control of Copper(I)–Dioxygen Reactivity

Takao Osako,[a] Yoshimitsu Tachi,[a] Matsumi Doe,[a] Motoo Shiro,[b] Kei Ohkubo,[c] Shunichi Fukuzumi,*[c] and Shinobu Itoh*[a]

Abstract: Crystal structures of the copper(I) complexes $\mathbf{1^X}$, **2**, and **3** of a series of tridentate ligands $L1^X$, L2, and L3, respectively ($L1^X$: *p*-substituted derivatives of *N*,*N*-bis[2-(2-pyridyl)ethyl]-2-phenylethylamine; X = H, Me, OMe, Cl, NO_2; L2: *N*,*N*-bis[2-(2-pyridyl)ethyl]-2-methyl-2-phenylethylamine; L3: *N*,*N*-bis[2-(2-pyridyl)ethyl]-2,2-diphenylethylamine) were solved to demonstrate that all the copper(I) complexes involve an η^2 copper–arene interaction with the phenyl ring of the ligand sidearm. The Cu^I ion in each complex has a distorted tetrahedral geometry consisting of the three nitrogen atoms (one tertiary amine nitrogen atom and two pyridine nitrogen atoms) and C_1–C_2 of the phenyl ring of ligand sidearm, whereby the Cu–C distances of the copper–arene interaction significantly depend on the *para* substituents. The existence of the copper–arene interaction in a nonpolar organic solvent (CH_2Cl_2) was demonstrated by the observation of an intense MLCT band around 290 nm, and the magnitude of the interaction was evaluated by detailed analysis of the ^1H and ^{13}C NMR spectra and the redox potentials $E_{1/2}$ of the copper ion, as well as by means of the ligand-exchange reaction between the phenyl ring and CH_3CN as an external ligand. The thermodynamic parameters ΔH^o and ΔS^o for the ligand-exchange reaction with CH_3CN afforded a quantitative measure for the energy difference of the copper–arene interaction in the series of copper(I) complexes. Density functional studies indicated that the copper(I)–arene interaction mainly consists of the interaction between the d_{z^2} orbital of Cu^I and a π orbital of the phenyl ring. The copper(I) complexes $\mathbf{1^X}$ reacted with O_2 at $-80\,°C$ in CH_2Cl_2 to give the corresponding (μ-η^2:η^2-peroxo)dicopper(II) complexes **4**, the formation rates k_{obs} of which were significantly retarded by stronger d–π interaction, while complexes **2** and **3**, which exhibit the strongest d–π interaction showed significantly lower reactivity toward O_2 under the same experimental conditions. Thus, the d–π interaction has been demonstrated for the first time to affect the copper(I)–dioxygen reactivity, and represents a new aspect of ligand effects in copper(I)–dioxygen chemistry.

Keywords: copper · Pi interactions · N ligands · O–O activation · substituent effects

Introduction

Weak interactions such as hydrogen bonding, π–π stacking, cation–π, and CH–π interactions are recognized as essential tools in molecular recognition and supramolecular chemistry.[1–7] Such interactions play versatile roles not only in the structural regulation of molecular architectures but also in controlling their physicochemical properties and functions. Transition metal π complexes of aromatic compounds are also well known as important intermediates in a wide variety of catalytic reactions with industrial and synthetic applications.[8–10] For copper, however, structurally characterized arene complexes are relatively rare,[11–19] and very little is known about the physicochemical aspects of the copper–arene interaction.

Copper complexes of a wide variety of ligands have been developed, especially in the field of bioinorganic chemistry, to replicate the structures and functions of the active sites of

[a] T. Osako, Dr. Y. Tachi, M. Doe, Prof. S. Itoh
Department of Chemistry, Graduate School of Science, Osaka City University
3-3-138 Sugimoto, Sumiyoshi-ku, Osaka 558-8585 (Japan)
Tel/Fax: (+81) 6-6605-2564
E-mail: shinobu@sci.osaka-cu.ac.jp

[b] Dr. M. Shiro
X-ray Research Laboratory, Rigaku Agency
3-9-12 Matsubara, Akishima-shi, Tokyo 196-8666 (Japan)

[c] Dr. K. Ohkubo, Prof. S. Fukuzumi
Department of Material and Life Science, Graduate School of Engineering, Osaka University
CREST, Japan Science and Technology Corporation
2-1 Yamada-oka, Suita, Osaka 565-0871 (Japan)

Supporting information for this article is available on the WWW under http://www.chemeurj.org/ or from the author.

 DOI: 10.1002/chem.200305263

copper proteins (enzymes).[20] In particular, dioxygen activation by copper(I) complexes is an important and attractive research objective, not only in bioinorganic chemistry but also in catalytic oxidation reactions.[21–27] In recent years, extensive efforts have been devoted to clarifying the effects of ligands on the structure and reactivity of copper–dioxygen intermediates, and demonstrated that nitrogen-donor capability and denticity (didentate versus tridentate versus tetradentate), as well as steric effects of the supporting ligands, are crucial in controlling the structure and reactivity.[28–34] Recently, it was shown that the presence of acidic protons on the nitrogen donor atoms of the ligand alters the structure and stability of resulting Cu_2/O_2 complexes.[35,36] Since most of the ligands so far been employed contain aromatic groups, copper(I)–arene interactions may also play important roles in controlling the structure and reactivity of the copper(I) complexes toward dioxygen. However, little attention has been paid to copper(I)–arene interactions in copper(I)–dioxygen chemistry.[37]

We report herein the first quantitative evaluation of the d–π interaction in copper(I) complexes of a series of bis[2-(2-pyridyl)ethyl]amine tridentate ligands L1–L3. The crystal structures, spectroscopic features (NMR and UV/Vis), and redox behavior of the copper(I) complexes were systematically investigated to provide profound insights into the structure and physicochemical features of the copper(I)–arene interaction. Moreover, it was shown that the reactivity of the copper(I) complexes toward dioxygen is significantly influenced by the ligand substituents through the d–π interaction in the copper(I) starting materials.

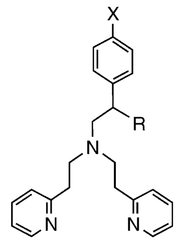

Ligand	R	X
$L1^{H}$	H	H
$L1^{OMe}$	H	OMe
$L1^{Me}$	H	Me
$L1^{Cl}$	H	Cl
$L1^{NO_2}$	H	NO_2
L2	Me	H
L3	Ph	H

Results and Discussion

Structural characterization of copper(I)--arene interactions: Crystal structures of $[Cu^I(L1^X)]ClO_4$ ($\mathbf{1^X}$, X = H, Me, OMe, Cl, and NO_2) and $[Cu^I(L3)]ClO_4$ (**3**) were determined (Figure 1), while that of $[Cu^I(L2)]ClO_4$ (**2**) was already reported in our previous paper.[19] The crystallographic data of $\mathbf{1^X}$ and **3** are presented in Table 1, and selected bond lengths around the copper ion are summarized in Table 2, in which the data of **2** are also included. It is noteworthy that the unit cell of $\mathbf{1^H}$ contains ten crystallographically independent molecules, and is thus an unusually long rectangular parallelepiped ($a = 15.695(2)$, $b = 78.34(1)$, $c = 17.389(4)$ Å), while the other complexes form normal unit

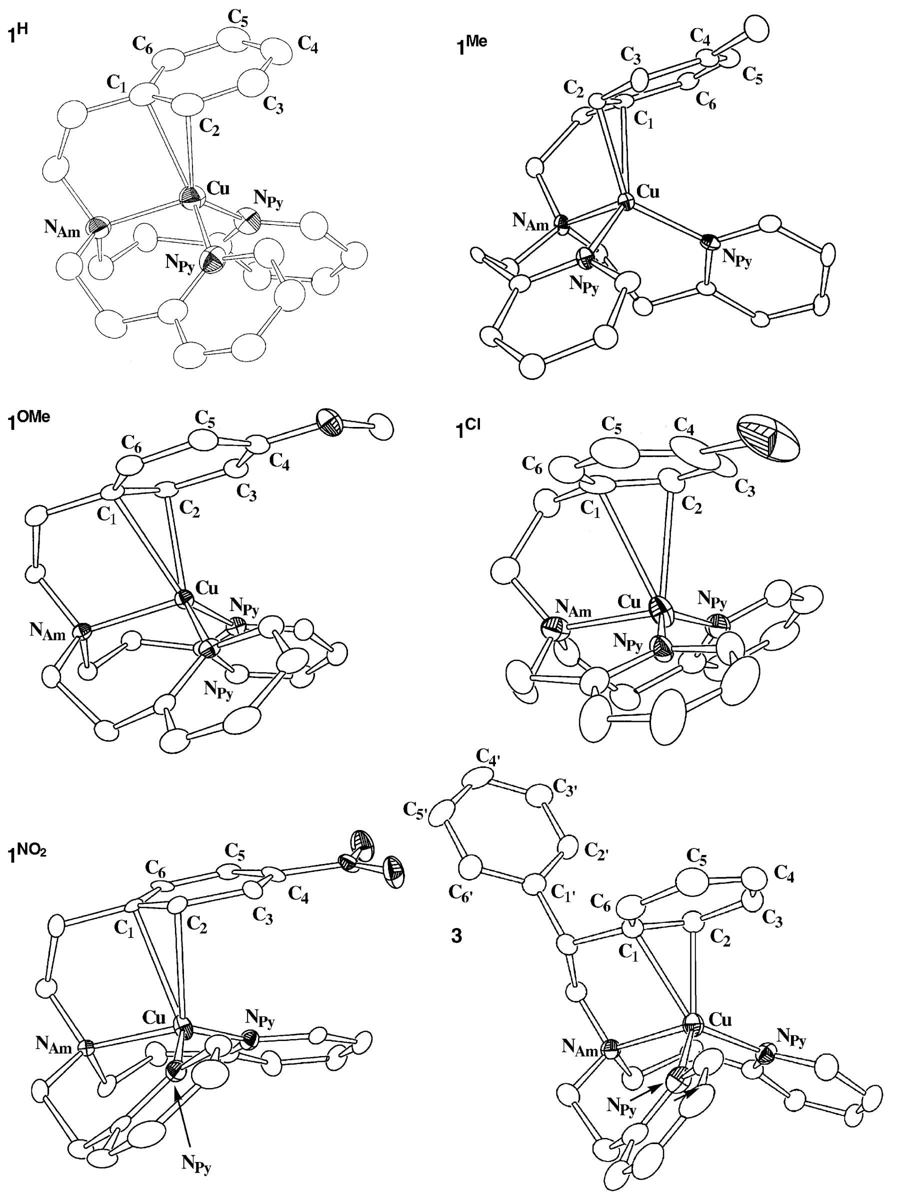

Figure 1. ORTEP plots of $\mathbf{1^X}$ (X = OMe, Me, H, Cl, NO_2) and **3** with 50% probability thermal ellipsoids The counteranion and hydrogen atoms are omitted for clarity.

www.chemeurj.org *Chem. Eur. J.* **2004**, *10*, 237–246

Table 1. Summary of X-ray crystallographic data.

	$[Cu^I(L1^H)]ClO_4$ (**1^H**)	$[Cu^I(L1^{Me})]ClO_4$ (**1^Me**)	$[Cu^I(L1^{OMe})]ClO_4$ (**1^OMe**)	$[Cu^I(L1^{Cl})]ClO_4$ (**1^Cl**)	$[Cu^I(L1^{NO_2})]ClO_4$ (**1^NO2**)	$[Cu^I(L3)]ClO_4$ (**3**)
empirical formula	$C_{22}H_{25}N_3O_3ClCu$	$C_{23}H_{27}N_3O_4ClCu$	$C_{23}H_{27}N_3O_5ClCu$	$C_{22}H_{24}N_3O_4Cl_2Cu$	$C_{22}H_{24}N_4O_6ClCu$	$C_{28}H_{29}N_3O_4ClCu$
formula weight	494.46	508.49	524.48	528.90	539.46	570.55
crystal system	monoclinic	orthorhombic	monoclinic	monoclinic	monoclinic	monoclinic
space group	$P2_1/a$ (no. 14)	$Pna2_1$ (no. 33)	$P2_1/n$ (no. 14)	$P2_1/n$ (no. 14)	$P2_1$ (no. 4)	$P2_1/n$ (no. 14)
a [Å]	15.695(2)	33.879(1)	9.9597(2)	12.6164(8)	12.6536(4)	8.6219(5)
b [Å]	78.34(1)	10.9386(4)	17.1256(5)	12.9552(9)	12.9535(5)	17.4195(9)
c [Å]	17.389(4)	11.9705(5)	13.3791(3)	15.007(1)	14.8924(6)	17.0987(8)
β [°]	90.73(2)	90	102.674(1)	111.821(2)	112.4000(5)	95.844(2)
V [$Å^3$]	21 380(6)	4436.1(2)	2226.41(8)	2277.1(3)	2256.8(1)	2554.7(2)
Z	40	8	4	4	4	4
$F(000)$	10 240.00	2112.00	1088.00	1088.00	1112.00	1184.00
ρ_{calcd} [$g\,cm^{-3}$]	1.536	1.523	1.565	1.543	1.588	1.483
T [°C]	−180	−115	−115	−115	−115	−115
crystal size [mm]	0.25×0.15×0.07	0.20×0.20×0.10	0.20×0.30×0.10	0.20×0.20×0.10	0.20×0.20×0.10	0.20×0.20×0.10
$\mu(Mo_{K\alpha})$ [cm^{-1}]	28.89	11.41	11.43	12.28	11.34	10.00
diffractometer	Rigaku RAXIS-RAPID	Rigaku RAXIS-RAPID	Rigaku RAXIS-RAPID	Rigaku RAXIS-RAPID	Rigaku RAXIS-RAPID	Rigaku RAXIS-RAPID
radiation	$Cu_{K\alpha}$ (λ = 1.54186 Å)	$Mo_{K\alpha}$ (λ = 0.71069 Å)	$Mo_{K\alpha}$ (λ = 0.71069 Å)	$Mo_{K\alpha}$ (λ = 0.71069 Å)	$Mo_{K\alpha}$ (λ = 0.71069 Å)	$Mo_{K\alpha}$ (λ = 0.71069 Å)
$2\theta_{max}$ [°]	136.5	55.0	55.0	55.0	55.0	54.9
no. of reflns measd	231 838	39 027	20 743	20 670	21 756	23 207
no. of reflns obsd	36 884 [$I > -3.00\sigma(I)$, $2\theta < 136.51°$]	5073 [$I > 0.01\sigma(I)$]	4179 [$I > 1.0\sigma(I)$]	3303 [$I > 0.5\sigma(I)$]	5205 [$I > 0.01\sigma(I)$]	4156 [$I > 1.0\sigma(I)$]
no. of variables	2791	632	326	314	662	364
R[a]	0.058	0.032	0.027	0.079	0.037	0.041
R_w[b]	0.141	0.076	0.039	0.103	0.049	0.076
GOF	1.12	0.98	0.89	1.34	0.96	0.82

[a] $R = \Sigma||F_o| - |F_c||/\Sigma|F_o|$. [b] $R_w = [\Sigma w(|F_o| - |F_c|)^2/\Sigma w(F_o^2)^2]^{1/2}$; $w = 1/\sigma^2(|F_o|)$.

Table 2. Selected bond lengths [Å] around the copper ion.[a]

Complex	$Cu–N_{amine}$	$Cu–N_{py}$	$Cu–C_1$	$Cu–C_2$
1^H	2.089	2.006	2.336	2.211
1^Me	2.114	2.013	2.359	2.207
1^OMe	2.098	1.992	2.514	2.195
1^Cl	2.137	1.972	2.656	2.476
1^NO2	2.115	1.967	2.597	2.388
2[b]	2.113	2.001	2.309	2.220
3	2.131	2.002	2.347	2.172

[a] Average values are presented where more than two crystallographically independent molecules exist in the unit cell. [b] Data are taken from the literature.[19]

cells containing one or two crystallographically independent molecules (Table 1 and Supporting Information: Figures S1–S6 and Tables S1–S6).

All the copper(I) complexes exhibit a similar type of copper(I)–arene interaction in the crystal, in which the phenyl ring of the ligand sidearm is positioned just above the copper(I) ion to undergo a coordinative interaction in a η^2 fashion (see Figure 1). Thus, the copper(I) ion in each complex adopts a distorted tetrahedral geometry consisting of the three nitrogen atoms (one N_{amine} and two N_{py}) and the C_1–C_2 moiety of the ligand sidearm. The η^2 bonding interaction is, however, significantly unsymmetrical, and the Cu–C_1 bond is always longer than the Cu–C_2 bond (Table 2).[38] Apparently, the Cu–C distances in the copper(I)–arene interaction largely depend on the *para* substituent X of the ligands, although the Cu–N distances are rather constant in the series ($d_{Cu-N(amine)} = 2.115 \pm 0.024$ Å; $d_{Cu-N(py)} = 1.990 \pm 0.023$ Å; Table 2). The Cu–C_2 bond lengths of **1^H**, **1^Me**, **1^OMe**, **2**, and **3** (2.172–2.211 Å) are shorter than those of **1^Cl** and **1^NO2** (2.476 and 2.388 Å), while the Cu–C_1 distances in **1^OMe**, **1^Cl**, and **1^NO2** (2.514–2.656 Å) are longer than those of **1^H**, **1^Me**, **2**, and **3** (2.309–2.359 Å). Thus, the difference in bond length between Cu–C_1 and Cu–C_2 is significantly larger in **1^OMe** than in the the other complexes. Crystal packing forces may influence the Cu–C bond lengths in the crystal. However, such an effect is relatively small, if any, since the differences in Cu–C_1 and Cu–C_2 bond lengths among the ten crystallographically independent molecules of **1^H** in the unit cell are relatively small (Cu–C_1 2.326 ± 0.069 Å, Cu–C_2 2.213 ± 0.035 Å). Thus, it can be concluded that the differences in the Cu–C bond lengths are mainly attributable to the difference in strength of the copper(I)–arene interaction. This issue is further examined below.

The C–C bond lengths of the phenyl rings of the copper(I) arene complexes are listed in Table S7 (Supporting Information), in which the corresponding values of another phenyl group in **3** without a copper(I)–arene interaction are also included. Overall, the copper(I)–arene interaction has little effect on the structure of the aromatic ring of the complexes.

The features of the copper(I)–arene interaction found in the crystal structures are well reproduced by the optimized structures obtained by DFT calculations (see Experimental Section).[39] Figure S7 (Supporting Information) shows the calculated structures of copper(I) arene complexes together with the Cu–C_1 and Cu–C_2 bond lengths. The calculated Cu–C_2 bond lengths are always shorter than the Cu–C_1 bond lengths, and the average Cu–C lengths $[(d_{Cu-C1}+d_{Cu-C2})/2]$ of **1^H^** and **1^Me^** are shorter than those of **1^OMe^**, **1^Cl^**, and **1^NO2^**, as was observed in the crystal structures (Figure 1). The larger difference in bond length between Cu–C_1 and Cu–C_2 in **1^OMe^** is also reproduced by the DFT calculation, but the calculated Cu–C_2 bond lengths of **1^Cl^** and **1^NO2^** are shorter than those in the crystal structures (Table 2). The interaction between the d_{z^2} orbital of Cu^I and the π orbital of the benzene ring is clearly seen at the HOMO-5 level of **1^H^** and **1^Me^**, as shown in Figure 2, where the Cu–C_2 interaction is much more evident than the Cu–C_1 interaction.

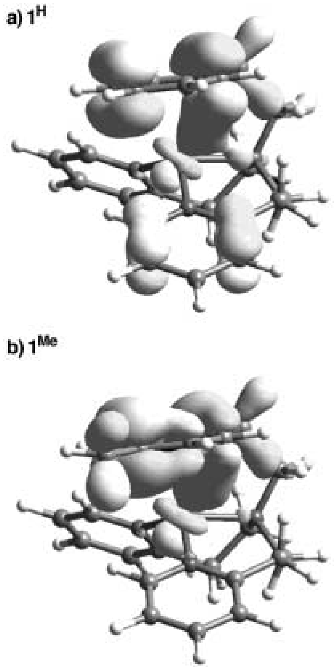

Figure 2. d–π orbital interaction of a) $\mathbf{1^H}$ and b) $\mathbf{1^{Me}}$, obtained by DFT calculation at the HOMO-5 level.

Copper(I)–arene interaction in solution: In the UV/Vis spectrum, the copper(I) complexes have a characteristic absorption band around 290 nm (ε = 7000–11 000 $M^{-1}cm^{-1}$) (Table 3). This absorption band can be assigned to metal-to-ligand charge transfer (MLCT) involving the phenyl group, since no such absorption band around 290 nm was observed for a similar copper(I) complex of a bis[2-(2-pyridyl)ethyl]-amine tridentate ligand without d–π interaction.[19] The absorption band around 290 nm disappeared when CH_3CN was added to a solution of the complex in CH_2Cl_2. A similar absorption band at 308 nm (ε = 18 000 $M^{-1}cm^{-1}$) in a Cu^I-η^2-indolyl complex, which disappeared on addition of CH_3CN, has also been assigned to a metal-to-indole charge-transfer transition.[18] This assignment is supported by the ^{13}C NMR chemical shifts of the aromatic carbon atoms of the ligand sidearm of $\mathbf{1^{Me}}$ in CD_2Cl_2, which are shifted to positions similar to those of the free ligand on addition of CD_3CN (Table 4). Further studies are required for detailed discussion of the MLCT transitions.

Table 3. UV/Vis and thermodynamic data for the titration of the copper(I) complexes with CH_3CN in CH_2Cl_2.

Complex	λ_{max} [nm]	ε [$M^{-1}cm^{-1}$]	K_{as}[a] [M^{-1}]	ΔH^o [$kJ mol^{-1}$]	ΔS^o [$J K^{-1} mol^{-1}$]
$\mathbf{1^H}$	290	8820	6.4±0.1	−12.4±1.6	−34±7
$\mathbf{1^{Me}}$	294	7000	8.6±0.1	−13.2±0.9	−35±4
$\mathbf{1^{OMe}}$	297	8520	12.2±0.1	−15.6±2.4	−42±10
$\mathbf{1^{Cl}}$	288	8190	30.3±0.2	−18.2±1.9	−44±8
$\mathbf{1^{NO_2}}$	287	–[b]	91.7±2.0	−20.6±0.5	−44±2
2	290[c]	9700[c]	0.21±0.01	−9.7±0.8	−52±3
3	289	11 000	0.10±0.02	−7.3±0.3	−48±2

[a] At −20 °C. [b] The ε value could not be determined accurately due to overlap with the strong absorption band of the nitro group in the ligand. [c] The data were taken from the literature.[19]

Figure 3 shows the spectral change in the titration of $\mathbf{1^{Me}}$ by CH_3CN in CH_2Cl_2 at −20 °C as a typical example. Disappearance of the absorption band at around 290 nm may be due to a ligand-exchange reaction between the aromatic ring and the added CH_3CN (Scheme 1), as demonstrated in the Cu^I–η^2-indolyl system.[18] The association constant of CH_3CN to the copper(I) complex $K_{as} = [Cu^IL \cdot CH_3CN]/[Cu^IL][CH_3CN]$ was determined to be 8.6±0.1 M^{-1} by analyzing the absorption change (inset of Figure 3), and the K_{as} values at −20 °C for all other complexes, determined by the

Table 4. ^{13}C NMR data of the aromatic group in the free ligands and the copper(I) complexes.[a]

		C_1	C_2 (C_6)	C_3 (C_5)	C_4
$L1^H$	δ_{ligand}[b]	141.37	129.18	128.57	126.12
	$\delta_{complex}$[c]	134.71	123.57	129.34	127.42
	$\Delta\delta$[d]	−6.66	−5.61	0.77	1.30
$L1^{Me}$	δ_{ligand}[b]	138.21	129.02	129.24	135.63
	$\delta_{complex}$[c]	131.75	123.43	129.89	137.36
	$\Delta\delta$[d]	−6.46	−5.59	0.65	1.73
	$\delta_{complex}$[e]	136.61	127.20	129.62	135.08
$L1^{OMe}$	δ_{ligand}[b]	133.36	130.03	113.98	158.30
	$\delta_{complex}$[c]	126.29	125.18	114.54	159.33
	$\Delta\delta$[d]	−7.07	−4.85	0.56	1.03
$L1^{Cl}$	δ_{ligand}[b]	140.11	130.67	128.51	131.66
	$\delta_{complex}$[c]	134.60	126.31	129.14	133.12
	$\Delta\delta$[d]	−5.51	−4.36	0.63	1.46
$L1^{NO_2}$	δ_{ligand}[b]	149.67	130.09	123.57	146.71
	$\delta_{complex}$[c]	147.18	127.12	123.91	144.49
	$\Delta\delta$[d]	−2.49	−2.97	0.34	−2.22
L2	δ_{ligand}[b]	146.95	127.72	128.53	126.22
	$\delta_{complex}$[c]	138.81	121.24	129.45	127.61
	$\Delta\delta$[d]	−8.14	−6.48	0.92	1.39
L3	δ_{ligand}[b]	144.53	128.63	128.62	126.45
	$\delta_{complex}$[c]	138.27	124.71	129.53	127.79
	$\Delta\delta$[d]	−6.26	−3.92	0.91	1.34

[a] In CD_2Cl_2. [b] Chemical shift of the free ligand. [c] Chemical shift of the copper(I) complex. [d] $\Delta\delta = \delta_{complex} - \delta_{ligand}$. [e] Chemical shifts of the aromatic carbon atoms of the ligand sidearm of $[Cu^IL1^{Me}]ClO_4$ (0.025 M) measured in CD_2Cl_2 containing CD_3CN (1.43 M) at 25 °C. Under these conditions, 18 % of the copper(I) complex retains the d–π interaction.

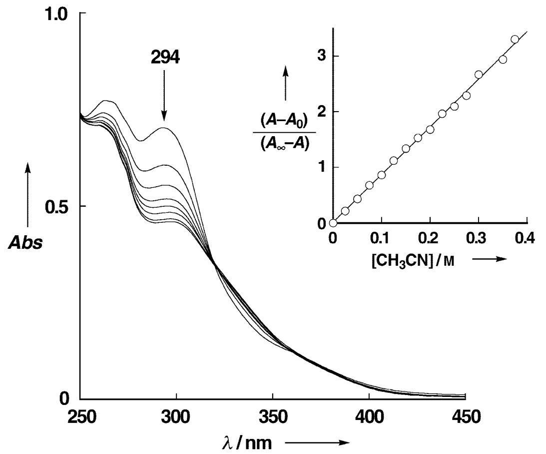

Figure 3. Spectral change in the titration of 1^{Me} (1.0×10^{-4} M) with CH_3CN at -20 °C in CH_2Cl_2. Inset: Plot of $(A-A_0)/(A_\infty-A)$ versus $[CH_3CN]$ based on the absorption change at 294 nm.

same method, are listed in Table 3. In addition, thermodynamic parameters ΔH^0 and ΔS^0 for the binding of CH_3CN to the copper(I) center were determined from the temperature dependence of K_{as} according to the equation $\ln K_{as} = -\Delta H^0/RT + \Delta S^0/R$ (Table 3 and Supporting Information, Figure S8).

The strength of CH_3CN–binding K_{as} can be evaluated from the ΔH^0 term, which reflects differences in the binding energy between CH_3CN and the phenyl ring to the copper(I) ion. Since the Cu–MeCN bond strength may be virtually the same in the CH_3CN complex (right species in Scheme 1) irrespective of the nature of X, the difference in ΔH^0 may directly reflect the energy difference in the copper(I)–arene interaction in the d–π complexes (left-hand side of Scheme 1), that is, the smaller the $-\Delta H^0$ value, the stronger the copper(I)–arene interaction. Apparently, the copper(I)–arene interaction is stronger in 1^H and 1^{Me} (smaller in K_{as}), while *para* OMe, Cl, and NO_2 substituents weaken the copper(I)–arene interaction in the series of 1^X. There is a compensating effect between ΔH^0 and ΔS^0. On the other hand, the methyl and phenyl groups at the benzylic position in **2** and **3** result in smaller $-\Delta H^0$ and larger $-\Delta S^0$ values. In the case of **2** and **3**, there is probably steric crowding due to the close proximity of R (Me and Ph) and the coordinated CH_3CN, which leads to the weaker binding. Thus, the K_{as} values of **2** and **3** are significantly smaller than those of 1^X. Then, the maximum energy difference reaches 13.3 kJ mol^{-1} between **3** and 1^{NO_2}.

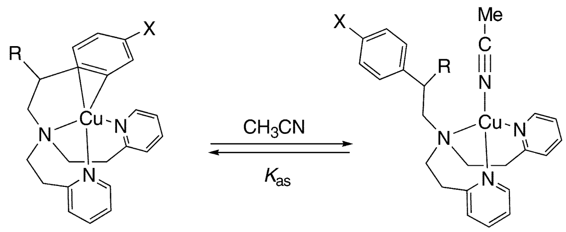

Scheme 1. Ligand exchange between the η^2-arene interaction and acetonitrile.

Studies by ^1H and ^{13}C NMR spectroscopy provided further insight into the copper(I)–arene interaction in solution. Assignment of all signals in the ^1H and ^{13}C NMR spectra was accomplished by employing 2D NMR techniques such as COSY, NOESY, HMQC, and HMBC, as summarized in the Experimental Section. The aromatic regions of the ^1H and ^{13}C NMR spectra of 1^{Me} in CD_2Cl_2 at 25 °C are shown in Figure 4 as typical examples. Apparently, the two ^1H and ^{13}C nuclei of the *ortho*- (2- and 6-) and *meta*- (3- and 5-) positions of the phenyl group of the ligand sidearm are magnetically equivalent. If the copper(I)--arene interaction in solution were fixed at the C_1–C_2 moiety, as in the crystal structure, the ^1H and ^{13}C nuclei in the 2- and 3-positions would give rise to different peaks from those of ^1H and ^{13}C at the 6- and 5-positions, respectively. Thus, the phenyl group is possibly swinging above the copper(I) ion as illustrated in Scheme 2, whereby the *ortho* (2- and 6-) and *meta* (3- and 5-) positions of the phenyl group become equivalent. The ^1H and ^{13}C NMR signals of the aromatic rings did not change at all, even at -80 °C, and this suggests that the energy barrier for the ring swinging above the copper(I) ion is very low.

Table 4 summarizes the ^{13}C NMR data of the aromatic groups of the free ligands and the corresponding copper(I) complexes. The copper(I)–arene interaction induces upfield shifts of the ^{13}C nuclei bound to the copper(I) ion [C_1 and C_2 (C_6)], while ^{13}C signals of C_3 (C_5) and C_4 exhibit downfield shifts, with the single exception of C_4 in $L1^{NO2}$. The upfield shifts of C_1 and C_2 (C_6) can be attributed to the electron-donating effect of the copper(I) ion through the d–π interaction. The electron-withdrawing substituents of 1^{Cl} and 1^{NO_2} resulted in smaller upfield shifts than for the other complexess, consistent with their weaker copper(I)–arene interactions.

The copper(I)–arene interaction was also examined by cyclic voltammetry in CH_2Cl_2. The copper(I) complexes exhibit a reversible or quasireversible redox couple due to one-electron oxidation/reduction of the copper center. A typical example of a cyclic voltammogram is shown in Figure 5, and the redox potentials ($E_{1/2}$ versus Fc/Fc^+) of all the copper(I) complexes are listed in Table 5. In this case, the $E_{1/2}$ values may reflect an inductive effect of the arene substituents, that is, the more strongly electron donating the substituent is, the more positive is the $E_{1/2}$ value in the series of 1^X.[40]

Copper(I)–dioxygen reactivity: In our previous study[41] copper(I) complex 1^H was shown to react with O_2 at a low temperature to give (μ-η^2:η^2-peroxo)dicopper(II) complex **4**, a model compound for the active oxygen intermediate of hemocyanin, tyrosinase, and catechol oxidase (Scheme 3).[42]

Oxygenation reactions of other copper(I) complexes 1^X (X = Me, OMe, Cl, and NO_2) were examined under the same experimental conditions (at -80 °C in CH_2Cl_2). The copper(I) complexes 1^X reacted with O_2 to give an oxygenated intermediate which was ESR-silent and gave essentially the same absorption spectrum as that of the (μ-η^2:η^2-peroxo)dicopper(II) complex derived from 1^H ($\lambda_{max} = 364$ nm).[41]

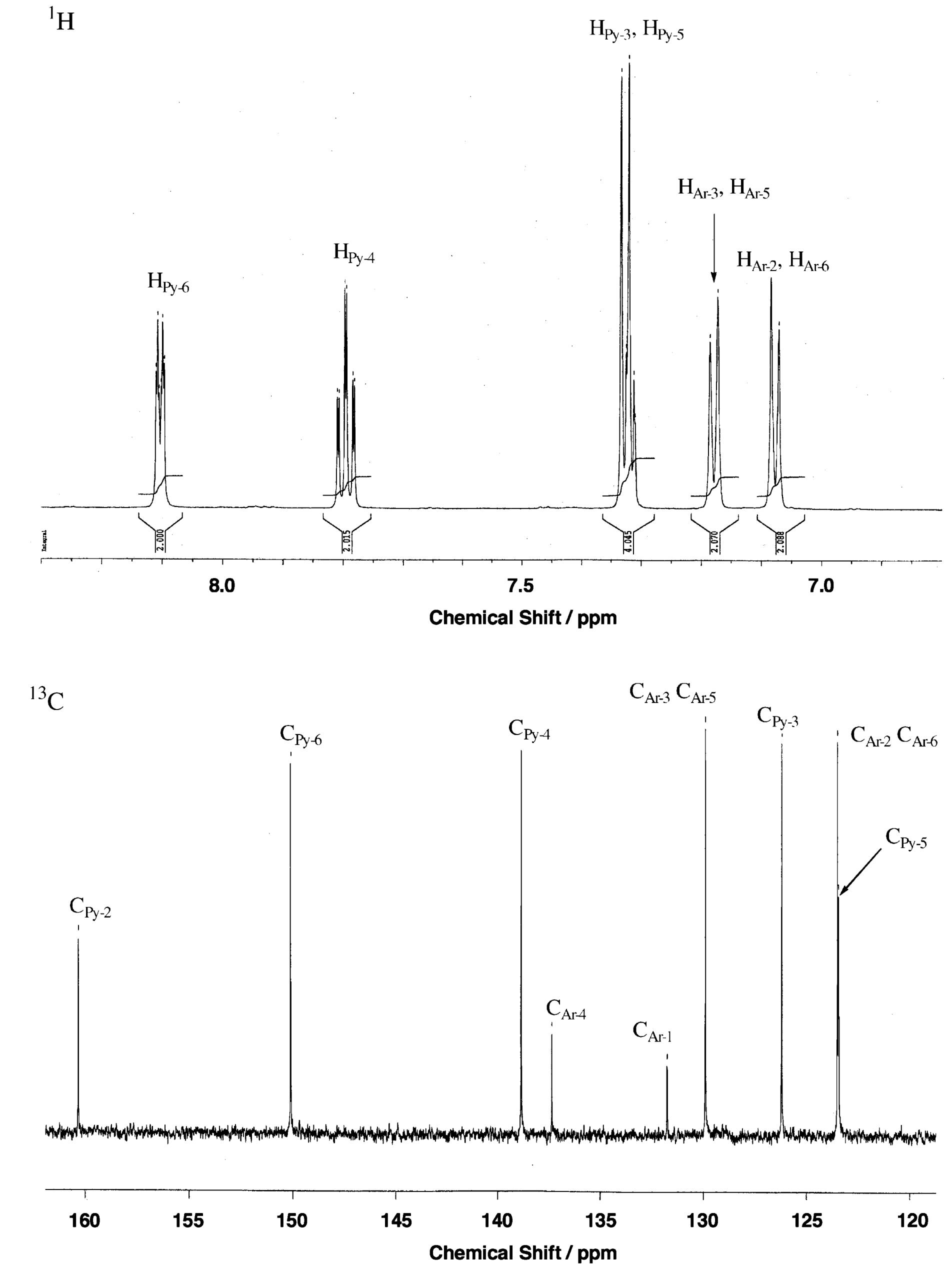

Figure 4. ^{1}H and ^{13}C NMR (aromatic region) of $\mathbf{1^{Me}}$ in CD_2Cl_2.

These features are strong evidence for the formation of (μ-η^2:η^2-peroxo)dicopper(II) complexes **4** in all cases. Interestingly, however, the formation rate k_{obs} of the peroxo intermediate depended significantly on the para substituent X of $L1^X$, and the copper(I) complexes **2** and **3** exhibited significantly lower reactivity toward O_2 under the same experimental conditions (Table 5).[19] Thus, the reactivity of the copper(I) complexes toward O_2 is significantly altered by the ligand substituents R and X. More importantly, the trend in formation rates k_{obs} of the peroxo intermediates **4** is very similar to that of K_{as}, that is, the stronger the copper(I)–arene interaction, the lower is the reactivity of $\mathbf{1^X}$ towards dioxygen. Thus, it is concluded that the interaction between O_2 and Cu^I is significantly affected by the *para* substituents X and the benzylic substituents R via the copper(I)–arene interaction.

Summary: The d–π interaction in copper(I) complexes of a series of bis[2-(2-pyridyl)ethyl]amine tridentate ligands has been systematically investigated for the first time by X-ray crystallographic analysis, UV/Vis and 2D-NMR spectroscopy, cyclic voltammetry, and DFT calculations. It is suggested that the interaction involves the d_{z^2} orbital of copper(I) and a π orbital of the arene ring, whereby the copper(I) ion acts as an electron donor. Thus, the interaction between the d orbital of Cu^I and the aromatic π orbital is stronger when the *para* substituent X is an electron-donating group such as H or Me, while electron-withdrawing substituents such as Cl and NO_2 weaken the overlap of the two orbitals. In the case of OMe, the situation is somewhat complicated, since the methoxyl group has both π-donor capability and a σ-electron-withdrawing effect, especially on the position *meta* to X (C_2). Overall, the OMe group may act as a σ-electron acceptor, weakening the d–π interaction to some extent. Further studies are required to obtain more detailed insight into the substituent effects on the copper(I)-arene interaction.

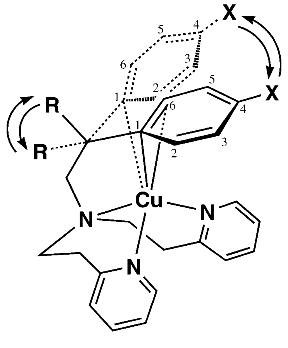

Scheme 2. Swinging of the phenyl ring in the copper(I) arene complex.

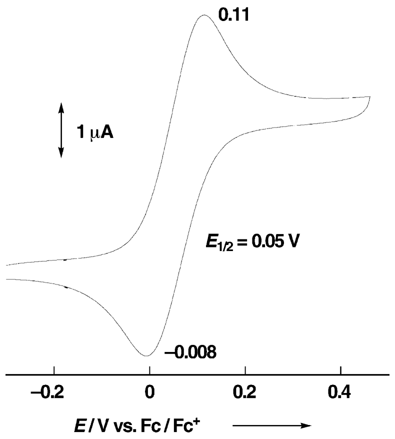

Figure 5. Cyclic voltammogram of $[Cu^I(L1^{Me})]ClO_4$ ($\mathbf{1^{Me}}$, 2.0×10^{-3} M) in CH_2Cl_2 containing 0.1 M TBAP; working electrode Pt, counter electrode Pt, pseudo-reference electrode Ag wire, scan rate 10 $mV\,s^{-1}$.

Table 5. Electrochemical data from cyclic voltammetry ($E_{1/2}$ and ΔE)[a] and the second-order rate constants k_{obs} for the formation of (μ-η^2:η^2-peroxo)dicopper(II) complexes **4**.[b]

Complex	$E_{1/2}$ [V] versus Fc/Fc$^+$	ΔE [V]	k_{obs} [$M^{-1}s^{-1}$]
$\mathbf{1^H}$	0.07	0.53	0.28 ± 0.01
$\mathbf{1^{Me}}$	0.05	0.12	0.70 ± 0.05
$\mathbf{1^{OMe}}$	0.05	0.18	1.96 ± 0.10
$\mathbf{1^{Cl}}$	−0.01	0.24	1.51 ± 0.06
$\mathbf{1^{NO_2}}$	−0.03	0.15	5.21 ± 0.30
2	0.16	0.17	–[c]
3	0.15	0.34	–[c]

[a] The electrochemical measurements were performed in CH_2Cl_2 containing 0.1 M tetrabutylammonium perchlorate (TBAP) at a scan rate of 10–50 $mV\,s^{-1}$ at 25 °C. [b] At −80 °C in CH_2Cl_2. [c] Very slow.

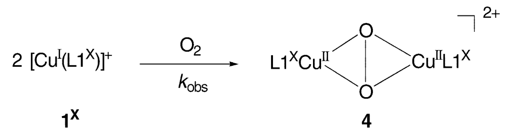

Scheme 3. Reaction of $\mathbf{1^X}$ with O_2.

Experimental Section

General: All chemicals used in this study, except for the ligands and the complexes, were commercial products of the highest available purity and were further purified by standard methods, if necessary.[43] Synthetic procedures for the ligands $L1^X$ and L3, except for $L1^{OMe}$, were reported previously.[19,41,44] FT-IR spectra were recorded with a Shimadzu FTIR-8200PC. UV/Vis spectra were measured with a Hewlett Packard HP8453 diode-array spectrophotometer with a Unisoku thermostatically controlled cell holder designed for low-temperature measurements (USP-203). Mass spectra were recorded with a JEOL JMS-700T Tandem MS station or a PE SCIEX API 150EX (for ESI-MS). NMR spectra were recorded on a Bruker Avance 600 spectrometer. ^{1}H NMR spectra were referenced to the residual proton resonance of the solvent, and ^{13}C NMR spectra to the solvent resonance (CD_2Cl_2: $\delta(^1H) = 5.32$, $\delta(^{13}C) = 53.8$). Complete peak assignments in the ^{1}H and ^{13}C NMR spectra of the ligands and the copper(I) complexes were accomplished by employing 2D NMR techniques (COSY, NOESY, HMQC, and HMBC). Cyclic voltammetry (CV) was performed on an ALS-630A electrochemical analyzer in anhydrous CH_2Cl_2 containing 0.1 M NBu_4ClO_4 (TBAP) as supporting electrolyte. The Pt working electrodes were polished with an alumina polishing suspension and rinsed with CH_2Cl_2 before use. The counterelectrode was a Pt wire. A silver pseudoreference electrode was used, and the potentials were determined relative to ferrocene/ferricenium (Fc/Fc$^+$). All electrochemical measurements were carried out at 25 °C under an atmospheric pressure of Ar in a glove box (DBO-1KP, Miwa Co. Ltd.).

***N,N*-Bis[2-(2-pyridyl)ethyl]-2-(4-methyoxyphenyl)ethylamine ($L1^{OMe}$)** was prepared by reaction of 2-(4-methoxyphenyl)ethylamine (3.0 g, 20 mmol) and 2-vinylpyridine (10.5 g, 100 mmol) in refluxing methanol (50 mL) containing acetic acid (6.0 g, 100 mmol) for 10 d, and purified by column chromatography (SiO_2), as for other ligands reported previously.[41,44] Pale brown oil (54.3 % yield); FAB-HRMS (positive ion): *m/z*: 362.227 [*M*+1].

$L1^H$: ^{1}H NMR (600 MHz, CD_2Cl_2, 27 °C): δ = 2.71 (dd, *J* = 10.3, 6.8 Hz, 2 H; NCH_2CH_2Ph), 2.80 (dd, *J* = 10.3, 6.8 Hz, 2 H; NCH_2CH_2Ph), 2.89 (dd, *J* = 8.1, 5.6 Hz, 4 H; NCH_2CH_2Py), 2.97 (dd, *J* = 8.1, 5.6 Hz, 4 H; NCH_2CH_2Py), 7.06 (d, *J* = 7.7 Hz, 2 H; H_{Py-3}), 7.10 (ddd, *J* = 7.5, 4.9, 0.9 Hz, 2 H; H_{Py-5}), 7.14 (d, *J* = 7.0 Hz, 2 H; H_{Ph-2}, $H_{Ph-2'}$), 7.17 (t, *J* = 7.3 Hz, 1 H; H_{Ph-4}), 7.25 (t, *J* = 7.2 Hz, 2 H; H_{Ph-3} and $H_{Ph-3'}$), 7.55 (td, *J* = 7.5, 1.8 Hz, 2 H; H_{Py-4}), 8.49 ppm (ddd, *J* = 4.9, 1.8, 0.9 Hz, 2 H; H_{Py-6}); ^{13}C NMR (600 MHz, CD_2Cl_2, 27 °C): 34.12 (NCH_2CH_2Ph), 36.30 (NCH_2CH_2Py), 54.22 (NCH_2CH_2Py), 56.33 (NCH_2CH_2Ph), 121.34 (C_{Py-5}), 123.70 (C_{Py-3}), 126.12 (C_{Ph-4}), 128.57 (C_{Ph-3}) 129.18 (C_{Ph-2}), 136.41 (C_{Py-4}), 141.37 (C_{Ph-1}), 149.46 (C_{Py-6}), 161.27 ppm (C_{Py-2}).

$L1^{Me}$: ^{1}H NMR (600 MHz, CD_2Cl_2, 27 °C): δ = 2.30 (s, 3 H; CH_3), 2.67 (dd, *J* = 8.5 and 5.3 Hz, 2 H; NCH_2CH_2Ar), 2.77 (dd, *J* = 8.5, 5.3 Hz, 2 H; NCH_2CH_2Ar), 2.89 (dd, *J* = 8.1, 5.4 Hz, 4 H; NCH_2CH_2Py), 2.97 (dd, *J* = 8.1, 5.4 Hz, 4 H; NCH_2CH_2Py), 7.02 (d, *J* = 7.9 Hz, 2 H; H_{Ar-2}, $H_{Ar-2'}$), 7.05 (d, *J* = 7.5 Hz, 2 H; H_{Py-3}), 7.07 (d, *J* = 7.9 Hz, 2 H; H_{Ar-3}, $H_{Ar-3'}$), 7.09 (ddd, *J* = 7.7, 4.9, 1.0 Hz, 2 H; H_{Py-5}), 7.54 (td, *J* = 7.7, 1.9 Hz, 2 H; H_{Py-4}), 8.49 ppm (ddd, *J* = 4.9, 1.9, 1.0 Hz, 2 H; H_{Py-6}); ^{13}C NMR (600 MHz, CD_2Cl_2, 27 °C): 21.07 (OCH_3), 33.68 (NCH_2CH_2Ar), 36.46 (NCH_2CH_2Py), 54.26 (NCH_2CH_2Py), 56.44 (NCH_2CH_2Ar), 121.28 (C_{Py-5}), 123.65 (C_{Py-3}), 129.02 (C_{Ar-2}), 129.24 (C_{Ar-3}), 135.63 (C_{Ar-4}), 136.30 (C_{Py-4}), 138.21 (C_{Ar-1}), 149.51 (C_{Py-6}), 161.37 ppm (C_{Py-2}).

$L1^{OMe}$: ^{1}H NMR (600 MHz, CD_2Cl_2, 27 °C): δ = 2.65 (dd, *J* = 10.0, 7.1 Hz, 2 H; NCH_2CH_2Ar), 2.76 (dd, *J* = 10.0, 7.1 Hz, 2 H; NCH_2CH_2Ar), 2.89 (dd, *J* = 8.0, 5.4 Hz, 4 H; NCH_2CH_2Py), 2.97 (dd, *J* = 8.0, 5.4 Hz, 4 H; NCH_2CH_2Py), 3.77 (s, 3 H; OCH_3), 6.80 (dt, *J* = 8.7, 2.1 Hz, 2 H; H_{Ar-3}, $H_{Ar-3'}$), 7.05 (d, *J* = 7.7, 2.1 Hz, 2 H; H_{Ar-2}, $H_{Ar-2'}$), 7.06, (d, *J* = 7.7 Hz, 2 H; H_{Py-3}), 7.09 (ddd, *J* = 7.7, 4.9, 1.0 Hz, 2 H; H_{Py-5}), 7.55 (td, *J* = 7.7, 1.8 Hz, 2 H; H_{Py-4}), 8.50 ppm (ddd, *J* = 4.9, 1.8, 1.0 Hz, 2 H; H_{Py-6}); ^{13}C NMR (600 MHz, CD_2Cl_2, 27 °C): 33.25 (NCH_2CH_2Ar), 36.47 (NCH_2CH_2Py), 54.26 (NCH_2CH_2Py), 55.53 (OCH_3), 56.53 (NCH_2CH_2Ar), 113.98 (C_{Ar-3}), 121.27 (C_{Py-5}), 123.63 (C_{Py-3}), 130.03 (C_{Ar-2}), 133.36 (C_{Ar-1}), 136.28 (C_{Py-4}), 149.50 (C_{Py-6}), 158.30 (C_{Ar-4}), 161.37 ppm (C_{Py-2}).

$L1^{Cl}$: ^{1}H NMR (600 MHz, CD_2Cl_2, 27 °C): δ = 2.66 (dd, *J* = 7.8, 5.6 Hz, 2 H; NCH_2CH_2Ar), 2.76 (dd, *J* = 7.8, 5.6 Hz, 2 H; NCH_2CH_2Ar), 2.85 (dd, *J* = 7.9, 6.6 Hz, 4 H; NCH_2CH_2Py), 2.95 (dd, *J* = 7.9, 6.6 Hz, 4 H; NCH_2CH_2Py), 7.00 (d, *J* = 7.8 Hz, 2 H; H_{Py-3}), 7.03 (d, *J* = 8.4 Hz, 2 H; H_{Ar-2}, $H_{Ar-2'}$), 7.09 (ddd, *J* = 7.6, 4.9, 1.0 Hz, 2 H; H_{Py-5}), 7.20 (d, *J* = 8.4 Hz, 2 H; H_{Ar-3}, $H_{Ar-3'}$), 7.53 (td, *J* = 7.6, 1.9 Hz, 2 H; H_{Py-4}), 8.49 ppm (ddd, *J* = 4.9, 1.9, 1.0 Hz, 2 H; H_{Py-6}); ^{13}C NMR (600 MHz, CD_2Cl_2, 27 °C): 33.55 (NCH_2CH_2Ar), 36.44 (NCH_2CH_2Py), 54.20 (NCH_2CH_2Py), 56.06 (NCH_2CH_2Ar), 121.30 (C_{Py-5}), 123.66 (C_{Py-3}), 128.51 (C_{Ar-3}), 130.67 (C_{Ar-2}), 131.66 (C_{Ar-4}), 136.29 (C_{Py-4}), 140.11 (C_{Ar-1}), 149.52 (C_{Py-6}), 161.29 ppm (C_{Py-2}).

$L1^{NO_2}$: ^{1}H NMR (600 MHz, CD_2Cl_2, 27 °C): δ = 2.76–2.82 (m, 4 H; NCH_2CH_2Ar), 2.84 (dd, *J* = 7.7, 6.8 Hz, 4 H; NCH_2CH_2Py), 2.96 (dd, *J* = 7.7, 6.8 Hz, 4 H; NCH_2CH_2Py), 7.00 (d, *J* = 7.7 Hz, 2 H; H_{Py-3}), 7.09 (ddd, *J* = 8.7, 4.9, 0.9 Hz, 2 H; H_{Py-5}), 7.21 (d, *J* = 8.7 Hz, 2 H; H_{Ar-2}, $H_{Ar-2'}$), 7.53 (td, *J* = 7.7, 1.8 Hz, 2 H; H_{Py-4}), 8.03 (d, *J* = 8.7 Hz, 2 H; H_{Ar-3}, $H_{Ar-3'}$), 8.48 ppm (ddd, *J* = 4.9, 1.8, 0.9 Hz, 2 H; H_{Py-6}); ^{13}C NMR (600 MHz, CD_2Cl_2, 27 °C): 34.13 (NCH_2CH_2Ar), 36.37 (NCH_2CH_2Py), 54.07 (NCH_2CH_2Py), 55.50 (NCH_2CH_2Ar), 121.36 (C_{Py-5}), 123.57 (C_{Ar-3}), 123.64 (C_{Py-3}), 130.09 (C_{Ar-2}), 136.32 (C_{Py-4}), 146.71 (C_{Ar-4}), 149.67 (C_{Ar-1}), 149.54 (C_{Py-6}), 161.15 ppm (C_{Py-2}).

L2: ^{1}H NMR (600 MHz, CD_2Cl_2, 27 °C): δ = 1.15 (d, *J* = 6.9 Hz, 3 H; $NCH_2CH(CH_3)Ph$), 2.61 (dd, *J* = 12.8, 8.0 Hz, 1 H; $NCH_2CH(CH_3)Ph$), 2.71 (dd, *J* = 12.8, 8.0 Hz, 1 H; $NCH_2CH(CH_3)Ph$), 2.82–2.98 (m, 7 H;

$NCH_2CH(CH_3)Ph$, NCH_2CH_2Py, NCH_2CH_2Py), 7.00 (d, J=7.8 Hz, 2H; H_{Py-3}), 7.11 (ddd, J=7.5, 6.0, 0.9 Hz, 2H; H_{Py-5}), 7.16 (d, J=7.5 Hz, 2H; H_{Ph-2}, $H_{Ph-2'}$), 7.19 (t, J=7.5 Hz, 1H; H_{Ph-4}), 7.28 (t, J=7.5 Hz, 2H; H_{Ph-3}, $H_{Ph-3'}$), 7.54 (td, J=7.7, 1.9 Hz, 2H; H_{Py-4}), 8.52 ppm (d, J=4.2, Hz, 2H; H_{Py-6}); ^{13}C NMR (600 MHz, CD_2Cl_2, 27°C): 19.98 ($NCH_2CH(CH_3)Ph$), 36.08 (NCH_2CH_2Py), 38.79 ($NCH_2CH(CH_3)Ph$), 54.73 (NCH_2CH_2Py), 62.68 ($NCH_2CH(CH_3)Ph$), 121.33 (C_{Py-5}), 123.82 (C_{Py-3}), 126.22 (C_{Ph-4}), 127.72 (C_{Ph-2}), 128.53 (C_{Ph-3}), 136.46 (C_{Py-4}), 146.95 (C_{Ph-1}), 149.26 (C_{Py-6}), 161.28 ppm (C_{Py-2}).

L3: ^{1}H NMR (600 MHz, CD_2Cl_2, 27°C): δ=2.81 (dd, J=7.9, 6.8 Hz, 4H; NCH_2CH_2Py), 2.97 (dd, J=7.9, 6.8 Hz, 4H; NCH_2CH_2Py), 3.20 (d, J=7.7 Hz, 2H; NCH_2CHPh_2), 4.15 (t, J=7.7 Hz, 1H; NCH_2CHPh_2), 6.87 (d, J=7.8 Hz, 2H; H_{Py-3}), 7.08 (ddd, J=7.4, 4.9, 1.1 Hz, 2H; H_{Py-5}), 7.18 (tt, J=7.8, 1.3 Hz, 2H; H_{Ph-4}), 7.21 (dd, J=7.1, 1.3 Hz, 4H; H_{Ph-2}, $H_{Ph-2'}$), 7.26 (td, J=7.3, 1.9 Hz, 4H; H_{Ph-3}, $H_{Ph-3'}$), 7.49 (ddd, J=7.8, 7.4, 1.8 Hz, 2H; H_{Py-4}), 8.50 ppm (ddd, J=4.9, 1.8, 0.8 Hz, 2H; H_{Py-6}); ^{13}C NMR (600 MHz, CD_2Cl_2, 27°C): 35.95 (NCH_2CH_2Py), 50.17 (NCH_2CHPh_2), 54.49 (NCH_2CH_2Py), 60.19 (NCH_2CHPh_2), 121.24 (C_{Py-5}), 123.67 (C_{Py-3}), 126.45 (C_{Ph-4}), 128.62 (C_{Ph-3}), 128.63 (C_{Ph-2}), 136.27 (C_{Py-4}), 144.53 (C_{Ph-1}), 149.45 (C_{Py-6}), 161.28 ppm (C_{Py-2}).

Caution! The perchlorate salts prepared in this study are all potentially explosive and should be handled with care.

[Cu^I(L1^{OMe})]ClO$_4$ (1^{OMe}): L1^{OMe} (108.4 mg, 0.3 mmol) was treated with [Cu^I(CH$_3$CN)$_4$]ClO$_4$ (96.1 mg, 0.3 mmol) in CH_2Cl_2 (5 mL) under an Ar atmosphere. After stirring for 30 min at room temperature, insoluble material was removed by filtration. Addition of diethyl ether (100 mL) to the filtrate gave a pale yellow powder that precipitated on allowing the mixture to stand for several minutes. The supernatant was then removed by decantation, and the remaining pale yellow solid was washed with diethyl ether three times and dried (68% yield). All procedures were performed in a glove box (DBO-1 KP, Miwa Co. Ltd., [O$_2$]<0.1 ppm). ^{1}H NMR (600 MHz, CD_2Cl_2, 27°C): δ=2.73 (brm, 2H; NCH_2CH_2Ar), 2.8–3.3 (brm, 10H; NCH_2CH_2Ar, NCH_2CH_2Py, NCH_2CH_2Py), 3.77 (s, 3 H; OCH_3), 6.89 (d, J=8.4 Hz, 2H; H_{Ar-3}, $H_{Ar-3'}$), 7.11 (d, J=8.4 Hz, 2H; H_{Ar-2}, $H_{Ar-2'}$), 7.37, (br, 4H; H_{Py-3}, H_{Py-5}), 7.82 (brt, J=7.0 Hz, 2H; H_{Py-4}), 8.19 ppm (br, 2H; H_{Py-6}); ^{13}C NMR (600 MHz, CD_2Cl_2, 27°C): 32.49 (NCH_2CH_2Ar), 34.04 (NCH_2CH_2Py), 54.56 (NCH_2CH_2Py), 55.88 (OCH_3), 56.28 (NCH_2CH_2Ar), 114.54 (C_{Ar-3}), 123.59 (C_{Py-5}), 125.18 (C_{Ar-2}), 126.64 (C_{Py-3}), 126.29 (C_{Ar-1}), 138.86 (C_{Py-4}), 150.13 (C_{Py-6}), 159.33 (C_{Ar-4}), 160.43 ppm (C_{Py-2}); FT-IR (KBr): $\tilde{\nu}$=1247, 1028 (OCH_3) 1115, 1089, 625 cm^{-1} (ClO_4^-); ESI-MS (positive ion), m/z: 424.0 [M^+]; elemental analysis (%) calcd for $C_{23}H_{27}O_5N_3CuCl$: C 52.67, H 5.19, N 8.01; found: C 52.38, H 5.23, N 7.95.

[Cu^I(L1^H)]ClO$_4$ (1^H): Synthetic procedure, mass spectrum, and elemental analysis of this compound were reported previously.[41] The NMR data recorded on a Bruker Avance 600 spectrometer in CD_2Cl_2 are as follows: ^{1}H NMR (600 MHz, CD_2Cl_2, 27°C): δ=2.82 (t, J=6.1 Hz, 2H; NCH_2CH_2Ph), 3.18 (t, J=6.1 Hz, 2H; NCH_2CH_2Ph), 2.8–3.2 (brm, 8H; NCH_2CH_2Py, NCH_2CH_2Py), 7.18 (d, J=7.5 Hz, 2H; H_{Ph-2} and $H_{Ph-2'}$), 7.30 (m, 2H; H_{Py-5}), 7.31 (t, J=7.5 Hz, 1H; H_{Ph-4}), 7.33 (d, J=7.8 Hz, 2 H; H_{Py-3}), 7.38 (t, J=7.5 Hz, 2H; H_{Ph-3}, $H_{Ph-3'}$), 7.79 (t, J=7.8, 1.8 Hz, 2H; H_{Py-4}), 8.08 ppm (d, J=4.1 Hz, 2H; H_{Py-6}); ^{13}C NMR (600 MHz, CD_2Cl_2, 27°C): 31.95 (NCH_2CH_2Ph), 34.03 (NCH_2CH_2Py), 54.54 (NCH_2CH_2Py), 56.02 (NCH_2CH_2Ph), 123.37 (C_{Py-3}), 123.57 (C_{Ph-2}), 127.40 (C_{Py-5}), 127.42 (C_{Ph-4}), 129.34 (C_{Phr-3}), 138.90 (C_{Py-4}), 134.71 (C_{Ph-1}), 150.23 (C_{Py-6}), 160.30 ppm (C_{Py-2}).

[Cu^I(L1^{Me})]ClO$_4$ (1^{Me}) was prepared in 56% yield in a similar manner to the synthesis of **1^{OMe}** by treating L1^{Me} (103.6 mg, 0.3 mmol) with [Cu^I(CH$_3$CN)$_4$]ClO$_4$ (96.1 mg, 0.3 mmol). All procedures were performed in a glove box ([O$_2$]< 0.1 ppm). ^{1}H NMR (600 MHz, CD_2Cl_2, 27°C): δ=2.32 (s, 3H; CH_3), 2.76 (t, J=6.0 Hz, 2H; NCH_2CH_2Ar), 3.15 (t, J=6.0 Hz, 2H; NCH_2CH_2Ar), 2.8–3.2 (brm, 8H; NCH_2CH_2Py, NCH_2CH_2Py), 7.08 (d, J=7.8 Hz, 2H; H_{Ar-2}, $H_{Ar-2'}$), 7.18 (d, J=7.8 Hz, 2 H; H_{Ar-3}, $H_{Ar-3'}$), 7.32 (td, J=7.8, 1.1 Hz, 2H; H_{Py-5}), 7.33 (d, J=7.8 Hz, 2 H; H_{Py-3}), 7.80 (td, J=7.8, 1.8 Hz, 2H; H_{Py-4}), 8.10 ppm (dt, J=7.8, 1.8 Hz, 2H; H_{Py-6}); ^{13}C NMR (600 MHz, CD_2Cl_2, 27°C): 21.12 (CH_3), 32.86 (NCH_2CH_2Ar), 32.98 (NCH_2CH_2Py), 54.55 (NCH_2CH_2Py), 56.38 (NCH_2CH_2Ar), 123.43 (C_{Ar-2}), 123.48 (C_{Py-5}), 126.18 (C_{Py-3}), 129.89 (C_{Ar-3}), 131.75 (C_{Ar-1}), 137.36 (C_{Ar-4}), 138.84 (C_{Py-4}), 150.10 (C_{Py-6}), 160.31 ppm (C_{Py-2}); FT-IR (KBr): $\tilde{\nu}$=1112, 1089, 625 cm^{-1} (ClO_4^-); ESI-MS (positive ion): m/z: 407.9 [M^+]; elemental analysis (%) calcd for $C_{23}H_{28}O_{4.5}N_3$·CuCl: C 53.38, H 5.45, N 8.12; found: C 53.61, H 5.42, N 8.00.

[Cu^I(L1^{Cl})]ClO$_4$ (1^{Cl}) was prepared in 59% yield in a similar manner to the synthesis of **1^{OMe}** by treating L1^{Cl} (109.8 mg, 0.3 mmol) with [Cu^I(CH$_3$CN)$_4$]ClO$_4$ (96.1 mg, 0.3 mmol). All procedures were performed in a glove box ([O$_2$]<0.1 ppm). ^{1}H NMR (600 MHz, CD_2Cl_2, 27°C): δ=2.77 (t, J=6.2 Hz, 2H; NCH_2CH_2Ar), 2.9–3.2 (brm, 10H; NCH_2CH_2Ar, NCH_2CH_2Py, NCH_2CH_2Py), 7.11 (d, J=8.1 Hz, 2H; H_{Ar-2} and $H_{Ar-2'}$), 7.30 (d, J=8.1 Hz, 2H; H_{Ar-3}, $H_{Ar-3'}$), 7.35–7.40 (m, 4H; H_{Py-3}, H_{Py-5}), 7.84 (t, J=7.5 Hz, 2H; H_{Py-4}), 8.22 ppm (br, 2H; H_{Py-6}); ^{13}C NMR (600 MHz, CD_2Cl_2, 27°C): 32.53 (NCH_2CH_2Ar), 34.35 (NCH_2CH_2Py), 54.68 (NCH_2CH_2Py), 56.27 (NCH_2CH_2Ar), 123.71 (C_{Py-5}), 126.31 (C_{Ar-2}), 126.37 (C_{Py-3}), 129.14 (C_{Ar-3}), 133.12 (C_{Ar-4}), 134.60 (C_{Ar-1}), 139.23 (C_{Py-4}), 150.36 (C_{Py-6}), 160.44 ppm (C_{Py-2}); FT-IR (KBr): $\tilde{\nu}$=1121, 1089, 625 cm^{-1} (ClO_4^-); ESI-MS (positive ion.): m/z: 428.0 [M^+]; elemental analysis (%) calcd for $C_{22}H_{24}O_4N_3CuCl_2$: C 49.96, H 4.57, N 7.94; found: C 49.92, H, 4.77, N, 7.61.

[Cu^I(L1^{NO_2})]ClO$_4$ (1^{NO_2}) was prepared in 68% yield in a similar manner to the synthesis of **1^{OMe}** by treating L1^{NO_2} (112.9 mg, 0.3 mmol) with [Cu^I(CH$_3$CN)$_4$]ClO$_4$ (96.1 mg, 0.3 mmol). All procedures were performed in a glove box ([O$_2$]<0.1 ppm). ^{1}H NMR (600 MHz, CD_2Cl_2, 27°C): δ=2.86 (t, J=7.0 Hz, 2H; NCH_2CH_2Ar), 3.05–3.15 (br, 8H; NCH_2CH_2Py), 3.07 (t, J=7.0 Hz, 2H; NCH_2CH_2Ar), 7.33 (d, J=8.6 Hz, 2H; H_{Ar-2}, $H_{Ar-2'}$), 7.38 (ddd, J=7.8, 5.4, 1.2 Hz, 2H; H_{Py-5}), 7.41 (d, J=7.8 Hz, 2H; H_{Py-3}), 7.87 (td, J=7.8, 1.8 Hz, 2H; H_{Py-4}), 8.11 (d, J=8.6 Hz, 2H; H_{Ar-3}, $H_{Ar-3'}$), 8.37 ppm (ddd, J=5.4, 1.8, 0.8 Hz, 2H; H_{Py-6}); ^{13}C NMR (600 MHz, CD_2Cl_2, 27°C): 32.88 (NCH_2CH_2Ar), 34.83 (NCH_2CH_2Py), 55.04 (NCH_2CH_2Py), 56.83 (NCH_2CH_2Ar), 123.86 (C_{Py-5}), 123.91 (C_{Ar-3}), 126.35 (C_{Py-3}), 127.12 (C_{Ar-2}), 139.53 (C_{Py-4}), 144.49 (C_{Ar-4}), 147.18 (C_{Ar-1}), 150.63 (C_{Py-6}), 160.58 ppm (C_{Py-2}); FT-IR (KBr): $\tilde{\nu}$=1514, 1345 (NO_2) 1113, 1089, 625 cm^{-1} (ClO_4^-); ESI-MS (positive ion): m/z: 439.0 [M^+]; elemental analysis (%) calcd for $C_{22}H_{25}O_{6.5}N_4CuCl$: C 48.18, H 4.59, N 10.22; found: C 48.41, H 4.50, N 10.07.

[Cu^I(L2)]ClO$_4$ (2): Synthetic procedure, mass spectrum, and elemental analysis of this compound were reported previously.[19] The NMR data recorded with a Bruker Avance 600 spectrometer in CD_2Cl_2 are as follows: ^{1}H NMR (600 MHz, CD_2Cl_2, 27°C): δ=1.20 (d, J=6.9 Hz, 3H; $NCH_2CH(CH_3)Ph$), 2.63 (dd, J=12.9, 4.2 Hz, 1H; $NCH_2CH(CH_3)Ph$), 2.75 (br, 1H; NCH_2CH_2Py), 2.80 (br, 1H; NCH_2CH_2Py), 2.85 (br, 1H; NCH_2CH_2Py), 2.93 (br, 1H; NCH_2CH_2Py), 2.95 (br, 1H; NCH_2CH_2Py), 2.98 (m, 1H; $NCH_2CH(CH_3)Ph$), 3.13 (brt, J=12.0 Hz, 1H; NCH_2CH_2Py), 3.23 (brt, J=14.6 Hz, 1H; NCH_2CH_2Py), 3.30 (brt, J=11.7 Hz, 1H; NCH_2CH_2Py), 3.44 (t, J=12.9 Hz, 1H; $NCH_2CH(CH_3)Ph$), 7.18 (d, J=7.6 Hz, 2H; H_{Ph-2}, $H_{Ph-2'}$), 7.21 (br, 1H; H_{Py-5}), 7.31 (br, 1H; H_{Py-3}), 7.33 (t, J=7.6 Hz, 1H; H_{Ph-4}), 7.36 (br, 1H; H_{Py-5}), 7.37 (br, 1H; H_{Py-3}), 7.39 (t, J=7.6 Hz, 2H; H_{Ph-3}, $H_{Ph-3'}$), 7.76 (br, 1H; H_{Py-4}), 7.80 (br, 1H; H_{Py-4}), 7.94 (br, 1H; H_{Py-6}), 8.04 ppm (br, 1H; H_{Py-6}); ^{13}C NMR (600 MHz, CD_2Cl_2, 27°C): 20.93 ($NCH_2CH(CH_3)Ph$), 33.63 (NCH_2CH_2Py), 33.98 (NCH_2CH_2Py), 38.96 ($NCH_2CH(CH_3)Ph$), 55.33 (NCH_2CH_2Py), 62.45 ($NCH_2CH(CH_3)Ph$), 121.24 (C_{Ph-2}), 123.37 (C_{Py-5}), 123.66 ($C_{Py-5'}$), 126.04 (C_{Py-3}), 126.25 ($C_{Py-3'}$), 127.61 (C_{Ph-4}), 129.45 (C_{Ph-3}), 138.81 (C_{Ph-1}), 138.96 (C_{Py-4}), 149.87 (C_{Py-6}), 150.28 ($C_{Py-6'}$), 160.27 ppm (C_{Py-2}).

[Cu^I(L3)]ClO$_4$ (3) was prepared in 67% yield in a similar manner to the synthesis of **1^{OMe}** by treating L3 (203.8 mg, 0.5 mmol) with [Cu^I(CH$_3$CN)$_4$]ClO$_4$ (160.1 mg, 0.5 mmol). All procedures were performed in a glove box ([O$_2$]<0.1 ppm). ^{1}H NMR (600 MHz, CD_2Cl_2, 27 °C): δ=2.90 (br, 2H; NCH_2CH_2Py), 3.08 (br, 2H; NCH_2CH_2Py), 3.15 (br, 4H; NCH_2CH_2Py, NCH_2CH_2Py), 3.38 (d, J=8.6 Hz, 2H; NCH_2CHPh_2), 4.20 (t, J=8.6 Hz, 1H; NCH_2CHPh_2), 7.23 (br, 2H; H_{Ph-4}), 7.29 (m, 2H; H_{Py-5}), 7.32 (m, 4H; H_{Ph-2}, $H_{Ph-2'}$), 7.35 (br, 4H; H_{Ph-3}, $H_{Ph-3'}$), 7.37 (m, 2H; H_{Py-3}), 7.81 (td, J=7.8, 1.8 Hz, 2H; H_{Py-4}), 7.95 ppm (ddd, J=5.3, 0.9, 0.6 Hz, 2H; H_{Py-6}); ^{13}C NMR (600 MHz, CD_2Cl_2, 27°C): 33.80 (NCH_2CH_2Py), 49.41 (NCH_2CHPh_2), 54.79 (NCH_2CH_2Py), 60.44 (NCH_2CHPh_2), 123.64 (C_{Py-5}), 124.71 (C_{Ph-2}), 126.30 (C_{Py-3}), 127.79 (C_{Ph-4}), 129.53 (C_{Ph-3}), 138.27 (C_{Ph-1}), 138.98 (C_{Py-4}), 150.13 (C_{Py-6}), 160.27 ppm (C_{Py-2}); FT-IR (KBr): $\tilde{\nu}$=1115, 1089, 625 cm^{-1} (ClO_4^-); FAB-MS (positive ion): m/z: 470.1 [M^+]; elemental analysis for [Cu^I(L3)]ClO$_4$, calcd (%) for $C_{28}H_{29}O_4N_3CuCl$: C 58.94, H 5.12, N 7.36; found: C 58.68, H 5.04, N 7.29.

X-ray structure determination: Single crystals of the copper(I) complexes for X-ray structural analysis were obtained by vapor diffusion of diethyl ether into a solution of the complex in CH_2Cl_2. In the case of $[Cu^I(L1^{NO_2})]ClO_4$, a few drops of methanol were added to a solution of $[Cu^I(L1^{NO_2})]ClO_4$ in CH_2Cl_2. Single crystals were mounted on a CryoLoop (Hamptom Research Co.). X-ray diffraction data were collected by a Rigaku RAXIS-RAPID imaging plate two-dimensional area detector using graphite-monochromated $Mo_{K\alpha}$ radiation ($\lambda = 0.71070$ Å) to $2\theta_{max} = 55.0°$ or $Cu_{K\alpha}$ radiation ($\lambda = 1.54186$ Å) to $2\theta_{max} = 136.6°$. All crystallographic calculations, except for $[Cu^I(L1^H)]ClO_4$, were performed by using the Crystal Structure software package of the Rigaku Corporation and Molecular Structure Corporation (Crystal Structure: Crystal Structure Analysis Package version 2.0, Rigaku Corp. and Molecular Structure Corp., **2001**). The crystallographic calculation of $[Cu^I(L1^H)]ClO_4$ was performed by using the teXsan crystallographic software package of Molecular Structure Corporation (**1999**). Crystal structures except for $[Cu^I(L1^H)]ClO_4$ were solved by direct methods and refined by full-matrix least-squares methods using SIR-92. All non-hydrogen atoms and hydrogen atoms were refined anisotropically and isotropically, respectively. In the case of $[Cu^I(L1^H)]ClO_4$, the crystal structure was solved by direct methods and refined by full-matrix least squares using SHELX-97. All non-hydrogen atoms of $[Cu^I(L1^H)]ClO_4$ were refined anisotropically, but the hydrogen atoms were not refined. Selected bond lengths and angles are given in Supporting Information (Tables S1–S6), and the X-ray structure determination and details of the crystallographic data are deposited as a CIF file.

CCDC-213269–213274 contain the supplementary crystallographic data for this paper. These data can be obtained free of charge via www.ccdc.cam.ac.uk/conts/retrieving.html (or from the Cambridge Crystallographic Data Centre, 12 Union Road, Cambridge CB2 1EZ, UK; fax: (+44) 1223-336-033; or e-mail: deposit@ccdc.cam.ac.uk).

Kinetic measurements: The reactions of the copper(I) complexes with O_2 were carried out in a UV/Vis cell with 1 mm path length that was held in a Unisoku thermostatically controlled cell holder USP-203 (a desired temperature can be fixed within ±0.5 °C). After keeping the deaerated solution of the copper(I) complex (2.5×10^{-3} M) in the cell at a desired temperature for several minutes, dry dioxygen gas was continuously supplied by gentle bubbling from a thin needle. Formation of the (μ-η^2:η^2-peroxo)dicopper(II) complex was monitored by means of the increase in the absorption at 364 nm. The reactions obeyed second-order kinetics, and the second-order rate constants k_{obs} were obtained as the slopes of linear second-order plots of $(A-A_0)/\{(A_\infty-A)[Cu]_0\}$ versus time, where A_0 and A_∞ are the initial and final absorption at 364 nm and $[Cu]_0$ is the initial concentration of $\mathbf{1^X}$.

Theoretical calculations: Density functional calculations were performed on a COMPAQ DS20E computer using the Amsterdam Density Functional (ADF) program version 1999.02 developed by Baerends et al.[45] The electronic configurations of the molecular systems were described by an uncontracted triple-ζ Slater-type orbital basis set (ADF basis set V) with a single polarization function for each atom. Core orbitals were frozen through 1s (C, O, N), 2p (Cl), and 3p (Cu). The calculations were performed by using the local exchange-correlation potential by Vosko et al.[46] and the nonlocal gradient corrections by Becke[47] and Perdew[48] during the geometry optimizations. First-order scalar relativistic correlations were added to the total energy. Final geometries and energetics were optimized by using the algorithm of Versluis and Ziegler[49] provided in the ADF package and were considered converged when the changes in bond lengths between subsequent iterations fell below 0.01 Å.

Acknowledgment

This work was financially supported in part by Grants-in-Aid for Scientific Research (No. 15350105) from the Ministry of Education, Culture, Sports, Science and Technology, Japan and by Research Fellowships of Japan Society for the Promotion of Science for Young Scientists.

[1] *Chem. Rev.* **1997**, *97*, 1231–1734: Special issue on molecular recognition.
[2] J.-M. Lehn, *Supramolecular Chemistry*, VCH, Weinheim, **1995**.
[3] T. E. Creighton, *Proteins: Structures and Molecular Properties*, 2nd ed., Freeman, New York, **1993**.
[4] W. Saenger, *Principles of Nucleic Acid Structure*, Springer, Heidelberg, **1984**.
[5] D. A. Dougherty, *Science* **1996**, *271*, 163–168.
[6] M. Nishio, M. Hirota, Y. Umezawa, *The CH-π Interactions*, Wiley-VCH, New York, **1998**.
[7] O. Yamauchi, A. Odani, M. Takani, *J. Chem. Soc. Dalton Trans.* **2002**, 3411–3421.
[8] E. L. Muetterties, J. R. Bleeke, E. J. Wucherer, T. A. Albright, *Chem. Rev.* **1982**, *82*, 499–525.
[9] E. Maslowsky, Jr., *J. Chem. Educ.* **1993**, *70*, 980–984.
[10] G. W. Parshall, S. D. Ittel, *Homogeneous Catalysis: The Applications and Chemistry of Catalysis by Soluble Transition Metal Complexes*, 2nd ed., Wiley-Interscience, New York, **1992**.
[11] R. W. Turner, E. L. Amma, *J. Am. Chem. Soc.* **1966**, *88*, 1877–1882.
[12] M. B. Dines, P. H. Bird, *J. Chem. Soc. Chem. Commun.* **1973**, 12.
[13] P. F. Rodesiler, E. L. Amma, *J. Chem. Soc. Chem. Commun.* **1974**, 599–600.
[14] M. Pasquali, C. Floriani, A. Gaetani-Manfredotti, *Inorg. Chem.* **1980**, *19*, 1191–1197.
[15] H. Schmidbaur, W. Bublak, B. Huber, G. Reber, G. Müller, *Angew. Chem.* **1986**, *98*, 1108; *Angew. Chem. Int. Ed. Engl.* **1986**, *25*, 1089–1090.
[16] M. Niemeyer, *Organometallics* **1998**, *17*, 4649–4656.
[17] a) W. S. Striejewske, R. R. Conry, *Chem. Commun.* **1998**, 555–556; b) R. R. Conry, W. S. Striejewske, A. A. Tipton, *Inorg. Chem.* **1999**, *38*, 2833.
[18] Y. Shimazaki, H. Yokoyama, O. Yamauchi, *Angew. Chem.* **1999**, *111*, 2561–2563; *Angew. Chem. Int. Ed.* **1999**, *38*, 2401–2403.
[19] T. Osako, Y. Tachi, M. Taki, S. Fukuzumi, S. Itoh, *Inorg. Chem.* **2001**, *40*, 6604–6609.
[20] *Bioinorganic Chemistry of Copper* (Eds.: K. D. Karlin, Z. Tyeklár), Chapman & Hall, New York, **1993**.
[21] A. G. Blackman, W. B. Tolman in *Metal-Oxo and Metal-Peroxo Species in Catalytic Oxidations* (Ed.: B. Meunier), Springer, Berlin, **2000**, pp. 179–211.
[22] L. Que, Jr., W. B. Tolman, *Angew. Chem.* **2002**, *114*, 1160–1185; *Angew. Chem. Int. Ed.* **2002**, *41*, 1114–1137.
[23] M.-A. Kopf, K. D. Karlin in *Biomimetic Oxidations Catalyzed by Transition Metal Complexes* (Ed.: B. Meunier), Imperial College Press, London, **1999**, pp. 309–362.
[24] V. Mahadevan, R. J. M. K. Gebbink, T. D. P. Stack, *Curr. Opin. Chem. Biol.* **2000**, *4*, 228–234.
[25] S. Itoh, S. Fukuzumi, *Bull. Chem. Soc. Jpn.* **2002**, *75*, 2081–2095.
[26] E. I. Solomon, U. M. Sundaram, T. E. Machonkin, *Chem. Rev.* **1996**, *96*, 2563–2605.
[27] S. Schindler, *Eur. J. Inorg. Chem.* **2000**, 2311–2326.
[28] W. B. Tolman, *Acc. Chem. Res.* **1997**, *30*, 227–237.
[29] A. P. Cole, D. E. Root, P. Mukherjee, E. I. Solomon, T. D. P. Stack, *Science* **1996**, *273*, 1848–1850.
[30] V. Mahadevan, M. J. Henson, E. I. Solomon, T. D. P. Stack, *J. Am. Chem. Soc.* **2000**, *122*, 10249–10250.
[31] M. Taki, S. Teramae, S. Nagatomo, Y. Tachi, T. Kitagawa, S. Itoh, S. Fukuzumi, *J. Am. Chem. Soc.* **2002**, *124*, 6367–6377.
[32] D. J. E. Spencer, N. W. Aboelella, A. M. Reynolds, P. L. Holland, W. B. Tolman, *J. Am. Chem. Soc.* **2002**, *124*, 2108–2109.
[33] N. W. Aboelella, E. A. Lewis, A. M. Anne M. Reynolds, W. W. Brennessel, C. J. Christopher J. Cramer, W. B. Tolman, *J. Am. Chem. Soc.* **2002**, *124*, 10660–10661.
[34] H. Hayashi, S. Fujinami, S. Nagatomo, S. Ogo, M. Suzuki, A. Uehara, Y. Watanabe, T. Kitagawa, *J. Am. Chem. Soc.* **2000**, *122*, 2124–2125.
[35] H.-C. Liang, C. X. Zhang, M. J. Henson, R. D. Sommer, K. R. Hatwell, S. Kaderli, A. D. Zuberbühler, A. L. Rheingold, E. I. Solomon, K. D. Karlin, *J. Am. Chem. Soc.* **2002**, *124*, 4170–4171.

[36] L. M. Mirica, M. Vance, D. J. Rudd, B. Hedman, K. O. Hodgson, E. I. Solomon, T. D. P. Stack, *J. Am. Chem. Soc.* **2002**, *124*, 9332–9333.
[37] A copper(I)–arene interaction was proposed to influence the copper(I)–dioxygen reactivity in some instances (K. D. Karlin, M. S. Nasir, B. I. Cohen, R. W. Cruse, S. Kaderli, A. D. Zuberbühler, *J. Am. Chem. Soc.* **1994**, *116*, 1324–1336 and ref. [39]). However, it has never been proved.
[38] The Cu–C_2 distances of the copper(I) complexes are comparable to the Cu–C distances in known Cu^I-η^2-benzene complexes (2.09–2.30 Å)[11,12,15] and in the recently reported Cu^I-η^2-phenyl (2.07–2.30 Å),[16] Cu^I-η^2-naphthyl (2.13, 2.41 Å),[17] and Cu^I-η^2-indolyl (2.23, 2.27 Å)[18] complexes.
[39] DFT studies on a copper(I)–benzene system with various basis sets have been reported: T. K. Dargel, R. H. Hertwig, W. Koch, *Mol. Phys.* **1999**, *96*, 583–591.
[40] There is no copper–arene interaction in the copper(II) complex of $\mathbf{1^H}$: S. Itoh, T. Kondo, M. Komatsu, Y. Ohshiro, C. Li, N. Kanehisa, Y. Kai, S. Fukuzumi, *J. Am. Chem. Soc.* **1995**, *117*, 4714–4715.
[41] S. Itoh, H. Nakao, L. M. Berreau, T. Kondo, M. Komatsu, S. Fukuzumi, *J. Am. Chem. Soc.* **1998**, *120*, 2890–2899.
[42] N. Kitajima, K. Fujisawa, Y. Moro-oka, *J. Am. Chem. Soc.* **1989**, *111*, 8975–8976.
[43] D. D. Perrin, W. L. F. Armarego, D. R. Perrin, *Purification of Laboratory Chemicals*, 4th ed., Pergamon Press, Elmsford, New York, **1996**.
[44] T. Osako, S. Nagatomo, Y. Tachi, T. Kitagawa, S. Itoh, *Angew. Chem.* **2002**, *114*, 4501–4504; *Angew. Chem. Int. Ed.* **2002**, *41*, 4325–4328.
[45] a) E. J. Baerends, D. E. Ellis, P. Ros, *Chem. Phys.* **1973**, *2*, 41–51; b) B. te Velde, E. J. Baerends, *J. Comput. Phys.* **1992**, *99*, 84–98.
[46] S. H. Vosko, L. Wilk, M. Nusair, *Can. J. Phys.* **1980**, *58*, 1200–1211.
[47] A. D. Becke, *Phys. Rev. A* **1988**, *38*, 3098–3100.
[48] a) J. P. Perdew, *Phys. Rev. B* **1986**, *33*, 8822–8824; b) J. P. Perdew, *Phys. Rev. B* **1986**, *34*, 7406.
[49] L. Versluis, T. Ziegler, *J. Chem. Phys.* **1988**, *88*, 322–328.

Received: June 23, 2003 [F5263]